Letters

Remaining Useful Life Prediction of Power Electronic Devices With Physics-Informed Deep Learning and Sparse Data

Le Gao, Chaoming Liu, *Member, IEEE*, Yiping Xiao, Chunhua Qi, and Mingxue Huo

***Abstract*—Accurate remaining useful life (RUL) prediction of silicon carbide MOSFETs is essential for ensuring the reliability of power electronic systems, particularly under irradiation environments. However, most existing deep learning approaches rely on densely sampled degradation data, making them unsuitable for sparse-data conditions where degradation observations are limited. To address this limitation, we propose a physics-informed deep learning (PIDL) method designed for sparse RUL prediction. The proposed method integrates total ionizing dose-induced degradation mechanisms, specifically interface and oxide trapped charge accumulation, into a Transformer-based neural architecture via a customized physics-informed loss function. This loss explicitly penalizes deviations from ON-state resistance degradation trajectories, thereby embedding domain knowledge into the model training process. Subsequently, particle swarm optimization is employed to optimize the model hyperparameters. We benchmark our method against a baseline Transformer model without physics-informed components, using four evaluation metrics: mean absolute error (MAE), root-mean-square error (RMSE), coefficient of determination (R^2), and a composite score. Under 90% data sparsity conditions, the PIDL approach achieves 27.90% reduction in MAE, 26.51% in RMSE, and 22.90% in score, demonstrating substantial gains in predictive accuracy and reliability. These results highlight the potential of PIDL in addressing sparse-data conditions.**

***Index Terms*—Deep learning, physics-informed, remaining useful life (RUL) prediction, silicon carbide metal-oxide-semiconductor field-effect transistors (SiC MOSFET), sparse data, total ionizing dose (TID) irradiation.**

I. Introduction

SILICON carbide metal-oxide-semiconductor field-effect transistors (SiC MOSFETs), owing to their high breakdown voltage, low leakage current, and stable frequency characteristics, have been widely adopted in critical aerospace electronic equipment, such as spacecraft power supplies and converters [1].

Received 21 January 2025; revised 24 March 2025; accepted 21 April 2025. Date of publication 24 April 2025; date of current version 27 August 2025. This work was supported in part by the National Natural Science Foundation of China under Grant U2341222, Grant U2441248, Grant 12275061, and Grant 12075069 and in part by the Fund for State Key Laboratory under Grant 6142806230204. *(Corresponding author: Chaoming Liu.)*

Le Gao, Chaoming Liu, Chunhua Qi, and Mingxue Huo are with the School of Astronautics, Harbin Institute of Technology, Harbin 150006, China (e-mail: cmliu@hit.edu.cn).

Yiping Xiao is with the School of Materials Science and Engineering, Harbin Institute of Technology, Harbin 150006, China.

Color versions of one or more figures in this article are available at https://doi.org/10.1109/TPEL.2025.3563853.

Digital Object Identifier 10.1109/TPEL.2025.3563853

However, in space radiation environments, high-energy particles induce radiation damage in SiC MOSFETs, leading to gradual functional degradation [2]. Without real-time monitoring of SiC MOSFETs degradation status, electronic system performance may decline, potentially resulting in disastrous consequences for power conversion devices (e.g., power supplies for satellites and accelerators) [3], [4]. To ensure the safe and efficient operation of SiC MOSFETs and to schedule timely maintenance, it is essential to develop a reliable and accurate degradation model to predict the remaining useful life (RUL) of these devices [5]. Most conventional RUL prediction methods necessitate complete and dense monitoring of the degradation precursor variables [6], [7]. However, in radiation environments, it is often infeasible to continuously and intensively obtain precursors for each SiC MOSFET, leading to incomplete or sparse data.

Recently, the rapid advancement of physics-informed machine learning has introduced novel avenues for achieving physics-informed RUL prediction [8]. By integrating simplified physical equations or latent physical laws into machine learning models, these approaches train models through a combination of empirical data and physical constraints [9]. Although only recently introduced, this new paradigm has already attracted considerable attention and has been explored in numerous disciplines, including fluid mechanics, chemistry, geology, and power systems [10].

In summary, to address the challenge of lifetime prediction for SiC MOSFETs under radiation environments with sparse data, we propose a physics-informed deep learning (PIDL) method that integrates a physics-informed model of radiation-induced degradation with a deep learning framework. This integrated approach is employed to forecast the RUL of SiC MOSFETs. Through gamma irradiation experiments on SiC MOSFETs, the proposed method has been empirically verified to be both effective and superior. The primary contributions of this article are summarized as follows.

1) A PIDL framework is proposed for the accurate prediction of the RUL of SiC MOSFETs under sparse-data conditions.
2) A novel loss function is developed to explicitly embed physics-informed degradation mechanisms into a Transformer-based deep learning architecture.
3) Particle swarm optimization (PSO) is introduced to optimize the model hyperparameters, reducing the complexity and manual effort.

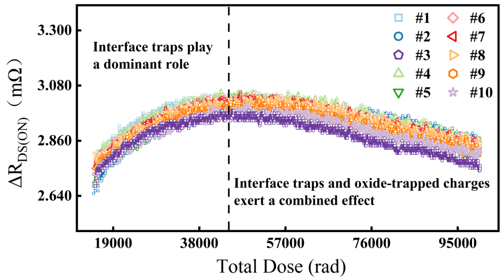

Fig. 1. Real-time variations in the ON-state resistance, $\Delta R_{DS(\text{ON})}$, recorded for SiC MOSFET devices under irradiation as a function of total dose.

The rest of this article is organized as follows. Section II introduces the degradation experiment and data collection. Section III elaborates on the proposed PIDL methodology. Section IV presents and discusses the results. Finally, Section V concludes this article.

II. Degradation Experiment and Data Collection

The radiation source employed in this study was ^{60}Co γ, providing a dose rate of 50 rad/s and a total dose of 100 krad (Si). In accordance with MIL-STD-883-1 and MIL-STD-750F, a constant gate voltage of $V_{GS} = 20$ V was applied to the device in this experimental setup. Furthermore, a transient pulsed current was introduced between the source and drain to measure the ON-state resistance ($R_{DS(\text{ON})}$).

As depicted in Fig. 1, real-time monitoring of device parameters under irradiation reveals that $\Delta R_{DS(\text{ON})}$ exhibits an initial increase, which is subsequently followed by a decrease. To mitigate manufacturing-related variations, $\Delta R_{DS(\text{ON})}$ was selected for analysis and subjected to noise reduction. This two-stage behavior reflects the interplay between interface trapped charges (negative) and oxide trapped charges (positive): the initial rise in $\Delta R_{DS(\text{ON})}$ is primarily driven by substantial oxide trapped charges and acceptor-like interface traps, which originate from hole trapping in bulk defects and interface reactions with precursor states. Because the rate of negatively charged interface-trap generation exceeds that of positively charged oxide trapped charges at low doses, interface traps dominate the early degradation process [11]. In line with previous findings [12], [13], this rapid formation of interface traps is attributed to the depassivation of carbon-related defects at low irradiation levels. As irradiation proceeds, oxide trapped charges progressively become the dominant factor, inducing a persistent negative shift in $\Delta R_{DS(\text{ON})}$.

In summary, the ON-state resistance of the SiC MOSFET device is selected as an indicator of impending failure under irradiation conditions. This parameter serves as the basis for constructing the subsequent physics-informed model and reflects the degradation of the gate oxide layer due to total ionizing dose (TID) effects, thereby representing the current degradation state of the device. To assess the performance of the proposed method under various incomplete data scenarios, we simulate multiple sparse-data conditions by sampling observations with varying levels of data sparsity. Specifically, observations from each device are randomly sampled at three predefined missing rates: 50%, 70%, and 90%. For example, a missing rate of 90% indicates that 90% of the observations are randomly removed from each device, leaving only 10% of the data available for model training.

III. Methodology

First, we establish a degradation model for $R_{DS(\text{ON})}$ due to TID effects in an irradiation environment. The key components affected by TID are the channel resistance R_{ch} and accumulation region resistance R_A, expressed as

$$R_{DS(\text{ON})} \approx R_{\text{ch}} + R_A = \frac{L_{\text{ch}}}{W_{\text{ch}}\mu_n C_{\text{ox}}(V_{GS} - V_{\text{th}})} + \frac{L_A}{W_A \mu_{nA} C_{\text{ox}}(V_{GS} - V_{\text{th}})} \quad (1)$$

where L_{ch} denotes the channel length, W_{ch} denotes the channel width, μ_n represents the electron mobility within the inversion layer channel of SiC, C_{ox} is the parasitic capacitance, L_A corresponds to the length of the accumulation region, W_A corresponds to the width of the accumulation region, μ_{nA} is the electron mobility of the accumulation layer, and V_{GS} is the gate drive voltage.

Considering the generation of interface-trapped (ΔV_{it}) and oxide-trapped (ΔV_{ot}) charges during irradiation

$$\Delta V_{\text{it}} = \frac{\Delta Q_{\text{it}}}{C_{\text{ox}}} = \frac{q T_{\text{ox}} A_{\text{it}} (\text{Dose})^{B_{\text{it}}}}{\varepsilon_{\text{ox}} A} \quad (2)$$

$$\Delta V_{\text{ot}} = -\frac{\Delta Q_{\text{ot}}}{C_{\text{ox}}} = -\frac{q T_{\text{ox}} A_{\text{ot}} (\text{Dose})^{B_{\text{ot}}}}{\varepsilon_{\text{ox}} A} \quad (3)$$

where q denotes the elementary charge, T_{ox} represents the oxide thickness, C_{ox} is the oxide capacitance, ε_{ox} signifies the permittivity of the oxide, A stands for the effective area, and Dose corresponds to the radiation dose. In these expressions, A_{it} and B_{it} are fitting parameters for the interface-trapped charge effect, whereas A_{ot} and B_{ot} pertain to the oxide-trapped charge effect.

We then integrate physical constraints from the degradation model of $\Delta R_{DS(\text{ON})}$ into the loss function of a machine learning model

$$\mathcal{L}(\theta) = w_{\text{dl}}\,\mathcal{L}_{\text{dl}}(\theta) + w_{\text{phy}}\,\mathcal{L}_{\text{phy}}(\theta) \quad (4)$$

where $w_{\text{dl}} + w_{\text{phy}} = 1$. The deep learning and physical losses are defined as

$$\mathcal{L}_{\text{dl}}(\theta) = \frac{1}{N_k}\sum_{j=1}^{N_k} \|\text{RUL}_p(x_{kj};\theta) - \Delta\text{RUL}_a(x_{kj};\theta)\|^2 \quad (5)$$

$$\mathcal{L}_{\text{phy}}(\theta) = \frac{1}{N_k}\sum_{i=1}^{N_k} \|\Delta R_p(x_{ki};\theta) - \Delta R_{\text{phy}}(x_{ki})\|^2 \quad (6)$$

where RUL_p and ΔR_p are predictions from the model at spatial coordinates x_{kj} and x_{ki}, respectively; ΔRUL_a and ΔR_{phy} denote actual and physically calculated values; N_k is the sample size for the kth device.

The final PIDL-based RUL prediction framework, as illustrated in Fig 2, integrates the PIDL framework with PSO. This integrated approach employs a sliding window method to extract

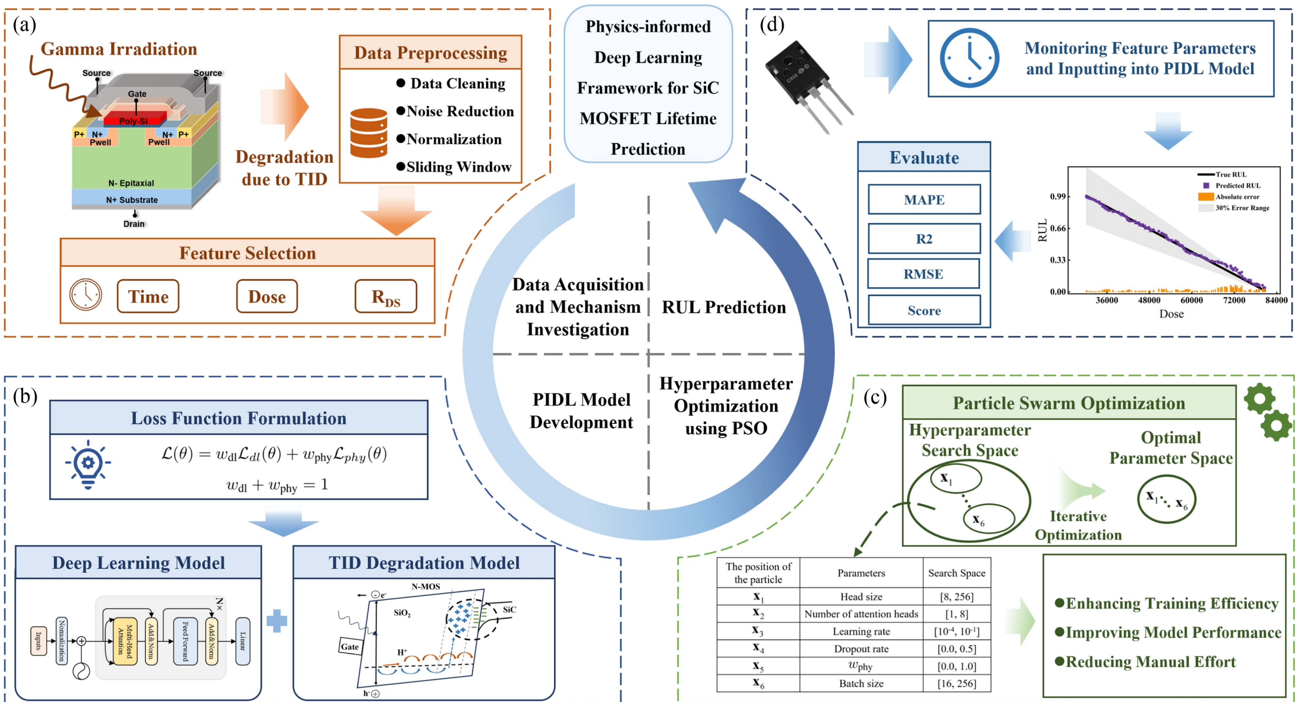

The position of the particle	Parameters	Search Space
x_1	Head size	[8, 256]
x_2	Number of attention heads	[1, 8]
x_3	Learning rate	[10^{-4}, 10^{-1}]
x_4	Dropout rate	[0.0, 0.5]
x_5	w_{phy}	[0.0, 1.0]
x_6	Batch size	[16, 256]

Fig. 2. Proposed PIDL-based RUL prediction framework. (a) Data acquisition and preprocessing. (b) Construction of the PIDL model. (c) Hyperparameter optimization via PSO. (d) RUL prediction.

temporal, dose, and resistance variation data across multiple devices. Subsequently, a Transformer model is utilized to output both the RUL and physical parameters, specifically $\Delta R_{\mathrm{DS(ON)}}$. Within this framework, physical modeling constraints are established by considering the contributions of interface traps and oxide charge capture. Furthermore, PSO is applied to adjust the model's hyperparameters, thereby achieving an optimal balance between data-driven learning and the preservation of physical information.

IV. Results and Discussion

A. Evaluation Metrics

In the context of RUL prediction, three widely recognized evaluation metrics—root-mean-square error (RMSE), mean absolute error (MAE), and the coefficient of determination (R^2)—are employed to rigorously assess the performance of various predictive methodologies. These three metrics are defined as follows:

$$\mathrm{RMSE} = \sqrt{\frac{1}{n}\sum_{i=1}^{n}(y_i - \hat{y}_i)^2} \tag{7}$$

$$\mathrm{MAE} = \frac{1}{n}\sum_{i=1}^{n}|y_i - \hat{y}_i| \tag{8}$$

$$R^2 = 1 - \frac{\sum_i (y_i - \hat{y}_i)^2}{\sum_i (y_i - \overline{y})^2} \tag{9}$$

where y_i and $\hat{y}_i$ represent the actual and predicted values at the ith data point, respectively, RMSE quantifies the square root of the average squared differences between predictions and actual values, while MAE measures the average magnitude of the absolute differences. Lower values of RMSE and MAE indicate a better predictive performance. In addition, the R^2 score, a statistical metric, serves as an alternative measure of the goodness of fit.

Concurrently, the Score metric is utilized to further evaluate the performance characteristics of RUL prediction models. This metric is specifically designed to account for the asymmetry in penalties for underestimation and overestimation [14], [15]. Late predictions are considered to pose significant risks, potentially leading to severe accidents, thus, late predictions are penalized more heavily than early predictions. In both cases, the penalty increases exponentially with the magnitude of the prediction error. The Score for experiment i is defined as follows:

$$\mathrm{Score} = \begin{cases} \frac{1}{N_k}\sum_{i=1}^{N_k}\left(e^{-\frac{d_i}{13}} - 1\right), & \text{for } d_i < 0 \\ \frac{1}{N_k}\sum_{i=1}^{N_k}\left(e^{\frac{d_i}{10}} - 1\right), & \text{for } d_i \geq 0 \end{cases} \tag{10}$$

where d_i denotes the prediction error, given by $d_i = y_i - \hat{y}_i$. A lower RUL score indicates that the model provides a more accurate estimation of the RUL.

B. RUL Prediction Results

In this section, we present the RUL prediction outcomes. The performance of the proposed PIDL model, referred to as physics-informed Transformer, was evaluated alongside that of a conventional deep learning model (Transformer). The evaluation was conducted under three distinct missing data rates—50%, 70%, and 90%—to simulate conditions of data sparsity.

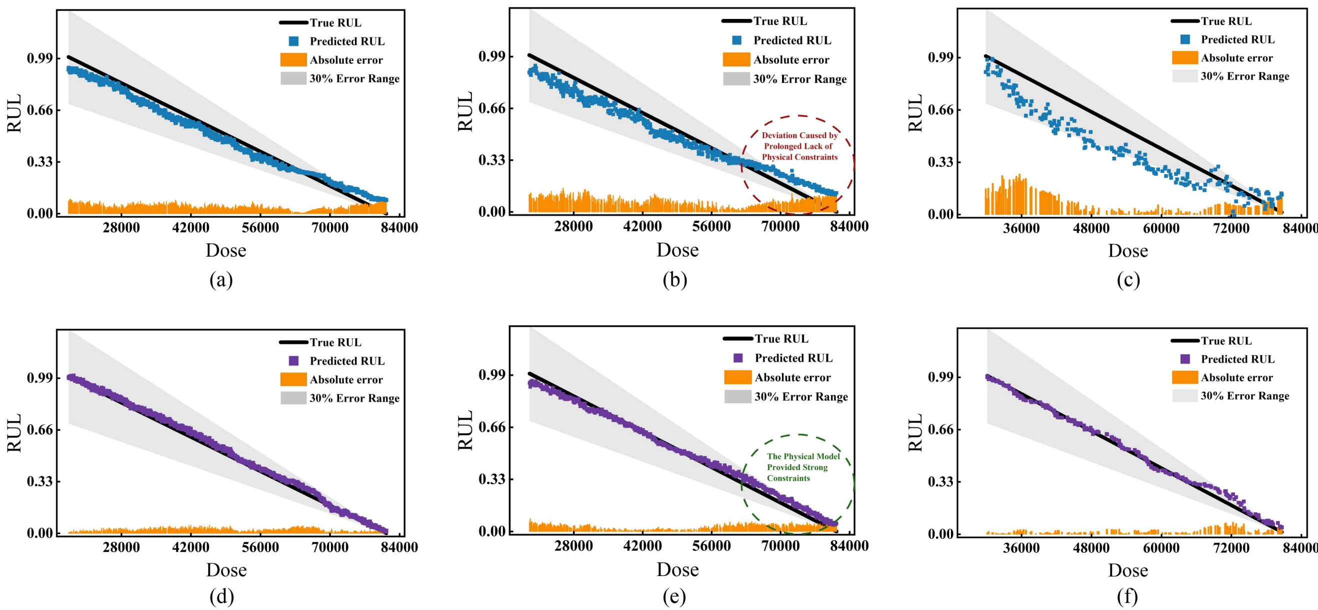

Fig. 3. Comparison of the RUL prediction performance and associated errors for both the Transformer model and the physics-informed Transformer model in the #10 device datasets under three different missing rates. (a) Transformer model at 50% missing rate. (b) Transformer model at 70% missing rate. (c) Transformer model at 90% missing rate. (d) Physics-informed Transformer model at 50% missing rate. (e) Physics-informed Transformer model at 70% missing rate. (f) Physics-informed Transformer model at 90% missing rate.

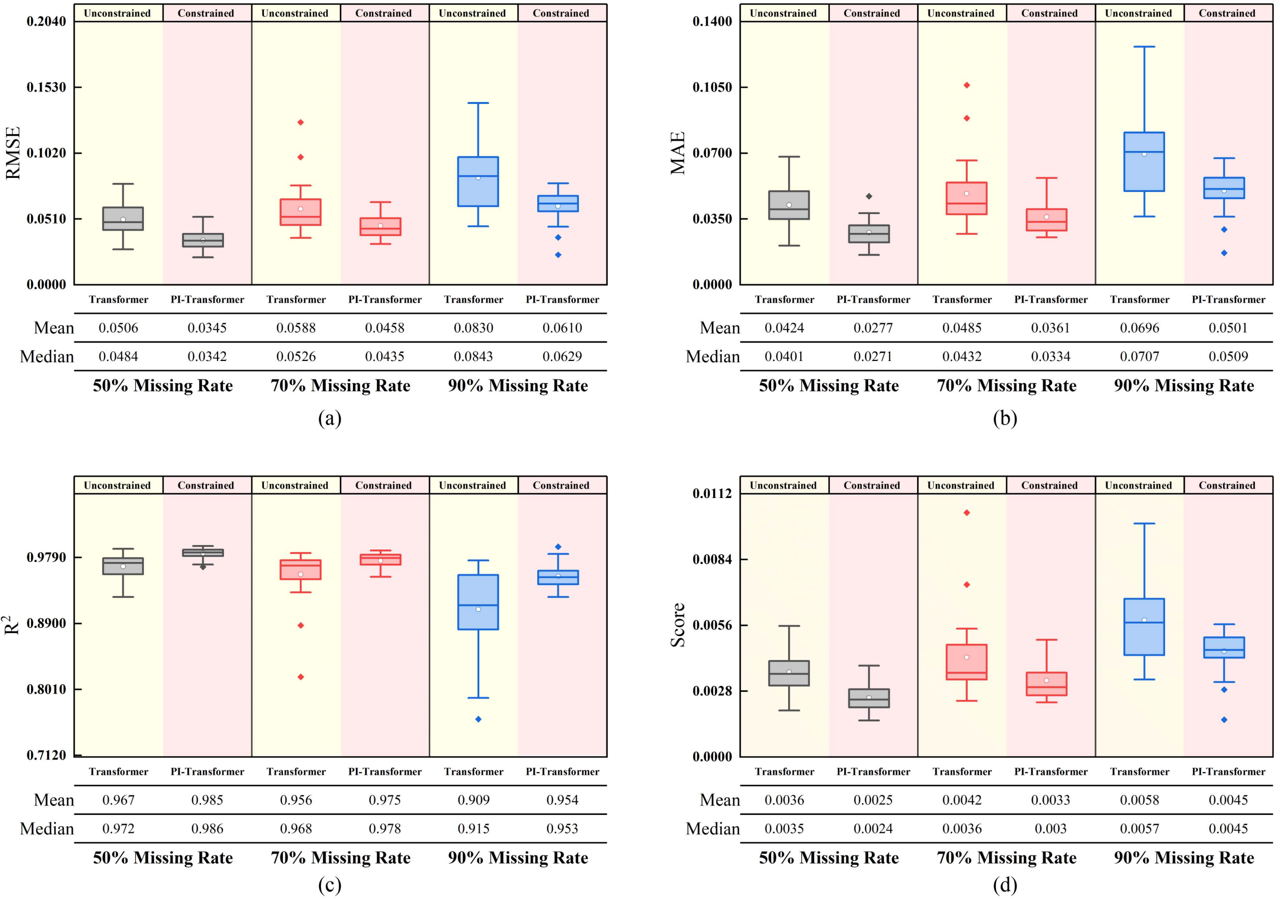

(a) RMSE

	Transformer	PI-Transformer	Transformer	PI-Transformer	Transformer	PI-Transformer
Mean	0.0506	0.0345	0.0588	0.0458	0.0830	0.0610
Median	0.0484	0.0342	0.0526	0.0435	0.0843	0.0629

(b) MAE

	Transformer	PI-Transformer	Transformer	PI-Transformer	Transformer	PI-Transformer
Mean	0.0424	0.0277	0.0485	0.0361	0.0696	0.0501
Median	0.0401	0.0271	0.0432	0.0334	0.0707	0.0509

(c) R^2

	Transformer	PI-Transformer	Transformer	PI-Transformer	Transformer	PI-Transformer
Mean	0.967	0.985	0.956	0.975	0.909	0.954
Median	0.972	0.986	0.968	0.978	0.915	0.953

(d) Score

	Transformer	PI-Transformer	Transformer	PI-Transformer	Transformer	PI-Transformer
Mean	0.0036	0.0025	0.0042	0.0033	0.0058	0.0045
Median	0.0035	0.0024	0.0036	0.003	0.0057	0.0045

Fig. 4. Box-and-whisker plots comparing the Transformer model and the physics-informed Transformer model across multiple runs under varying data loss rates. Four performance metrics are presented. (a) RMSE. (b) MAE. (c) R^2. (d) Score.

TABLE I
OVERALL PERFORMANCE COMPARISON OF THE PHYSICS-INFORMED TRANSFORMER MODEL AND TRANSFORMER MODEL UNDER VARYING DATA SPARSITY CONDITIONS

Sparsity Level	Physics-Informed Transformer model				Transformer model			
	RMSE	MAE	R^2	Score	RMSE	MAE	R^2	Score
50%	0.0345	0.0277	0.985	0.0025	0.0506	0.0424	0.967	0.0036
70%	0.0458	0.0361	0.975	0.0033	0.0588	0.0485	0.956	0.0042
90%	0.0610	0.0501	0.954	0.0045	0.0830	0.0696	0.909	0.0058

Reported values represent the average performance metrics obtained over multiple runs.

As illustrated in Fig. 3, we compare the specific trends in RUL prediction between the two models for device #10 across three missing-data rates. For clarity, the RUL values are normalized. From Fig. 3(a)–(c), it is evident that as the missing rate increases from 50% to 90%, the prediction deviation becomes increasingly pronounced, especially during later lifetime stages, with the absolute error eventually exceeding the 30% threshold (dashed lines). Absent is a physics-informed guiding framework, the deep learning model, that alone struggles to maintain forecasting accuracy in the face of incomplete data.

By contrast, in Fig. 3(d)–(f), the physics-informed Transformer—with strong physical constraints—consistently achieves low absolute error. Even at a 90% missing rate, its predictions remain well within the 30% error threshold, closely aligning with ground-truth values. This contrast demonstrates that purely data-driven approaches deteriorate markedly under sparse data conditions, whereas physics-guided methods exhibit robust predictive capability and reliability despite extensive data scarcity.

We further analyzed the performance of the physics-informed Transformer (constrained) and the conventional Transformer (unconstrained) across multiple runs, as depicted in Fig. 4. This box-and-whisker plot illustrates the statistical distribution of predictive outcomes for each method over repeated experiments, with the mean and median values shown below each box. Compared to the conventional Transformer, the proposed physics-informed Transformer exhibits consistently narrower distributions across all four evaluation metrics at different missing rates. In addition, both the mean and median of RMSE, MAE, and score remain lower for the physics-informed Transformer, and the variation in the box size does not expand significantly even as the missing rate increases. Hence, the incorporation of physical insights not only reduces the average prediction error but also enhances model stability.

Table I provides a comprehensive summary of these performance metrics. In conjunction with Fig. 4, the results indicate that at a 90% missing rate, the performance gap between the physics-informed Transformer and the conventional Transformer widens, with the RMSE reduced by approximately 26.51% and the MAE by about 27.90%. These findings confirm that physical constraints maintain high predictive accuracy under sparse-data conditions. Moreover, in terms of robustness and reliability, the R^2 values for the physics-informed Transformer remain above 0.95 for missing rates ranging from 50% to 90%. Notably, at a 90% missing rate, the R^2 of the proposed method surpasses that of the Transformer model by roughly 5%. Furthermore, the Score metric—an integrated measure of RUL prediction performance—decreases by 22.41%, reflecting a more comprehensive improvement in forecasted outcomes.

In summary, under varying levels of incomplete data, the proposed PIDL approach consistently demonstrates superior predictive accuracy, robustness, and overall reliability for RUL forecasting, affirming its suitability for specialized environments characterized by severe data sparsity.

V. CONCLUSION

This study addresses the challenge of predicting the RUL of SiC MOSFETs under sparse-data conditions in irradiation environments by proposing a PIDL framework. Specifically, a physics-informed model capturing oxide and interface trapped charges is embedded within a Transformer-based network, such that one branch focuses on RUL regression while another predicts pertinent physical variables. A PSO algorithm iteratively refines the deep learning hyperparameters and physical-model weighting coefficients, obviating the need for empirical tuning. Experimental results demonstrate that incorporating physical constraints enables effective interpretation of sparse datasets, improved long-range predictive accuracy, reduced uncertainty, and high-fidelity performance, particularly over extended prediction intervals; in doing so, the proposed method outperforms standard Transformer-based approaches. Beyond predicting the lifetime of SiC MOSFETs in irradiation settings, the framework generalizes to other devices and helps mitigate costs associated with downtime and failures. Nevertheless, like many deep learning techniques, the present approach primarily generates point predictions, underscoring the need for future investigations into uncertainty analysis and probability distributions of predicted RUL to enhance predictive confidence.

REFERENCES

[1] L. Wu et al., “Analysis of displacement damage induced by silicon-ion irradiation in SiC MOSFETs,” *IEEE Trans. Nucl. Sci.*, vol. 71, no. 7, pp. 1370–1379, Jul. 2024.

[2] Y. Xiao et al., “Ionization radiation-induced reliability degradation of SiC power MOSFET,” *IEEE Trans. Electron. Devices*, vol. 70, no. 12, pp. 6480–6485, Dec. 2023.

[3] L. Wu et al., “Impact of bias condition on electron radiation response of SiC MOSFETs,” *IEEE Trans. Nucl. Sci.*, vol. 72, no. 2, pp. 175–183, Feb. 2025.

[4] J.-M. Lauenstein, M. C. Casey, R. L. Ladbury, H. S. Kim, A. M. Phan, and A. D. Topper, “Space radiation effects on sic power device reliability,” in *Proc. IEEE Int. Rel. Phys. Symp.*, 2021, pp. 1–8.

[5] E. Zio, “Prognostics and health management (PHM): Where are we and where do we (need to) go in theory and practice,” *Rel. Eng. Syst. Saf.*, vol. 218, 2022, Art. no. 108119.

[6] M. Baharani, M. Biglarbegian, B. Parkhideh, and H. Tabkhi, "Real-time deep learning at the edge for scalable reliability modeling of Si-MOSFET power electronics converters," *IEEE Internet Things J.*, vol. 6, no. 5, pp. 7375–7385, Oct. 2019.

[7] Y. Hou et al., "Precursor prediction and early warning of power MOSFET failure using machine learning with model uncertainty considered," *IEEE J. Emerg. Sel. Top. Power Electron.*, vol. 12, no. 6, pp. 5762–5776, Dec. 2024.

[8] G. E. Karniadakis, I. G. Kevrekidis, L. Lu, P. Perdikaris, S. Wang, and L. Yang, "Physics-informed machine learning," *Nature Rev. Phys.*, vol. 3, no. 6, pp. 422–440, 2021.

[9] F. Jiang, X. Hou, and M. Xia, "Spatio-temporal attention-based hidden physics-informed neural network for remaining useful life prediction," *Adv. Eng. Informat.*, vol. 63, 2025, Art. no. 102958.

[10] Y. Fassi, V. Heiries, J. Boutet, and S. Boisseau, "Towards physics-informed machine learning-based predictive maintenance for power converters–a review," *IEEE Trans. Power Electron.*, vol. 39, no. 2, pp. 2692–2720, Feb. 2024.

[11] W.-H. Zhang et al., "Impact of low-dose radiation on nitrided lateral 4H-SiC MOSFETs and the related mechanisms," *Chin. Phys. B*, vol. 32, no. 5, 2023, Art. no. 057305.

[12] S. K. Dixit et al., "Total dose radiation response of nitrided and non-nitrided SiO_2/4H-SiC MOS capacitors," *IEEE Trans. Nucl. Sci.*, vol. 53, no. 6, pp. 3687–3692, Dec. 2006.

[13] T. Knežević, A. Hadžipašić, T. Ohshima, T. Makino, and I. Capan, "M-center in low-energy electron irradiated 4H-SiC," *Appl. Phys. Lett.*, vol. 120, no. 25, 2022, Art. no. 252101.

[14] L. Liu, X. Song, and Z. Zhou, "Aircraft engine remaining useful life estimation via a double attention-based data-driven architecture," *Rel. Eng. Syst. Saf.*, vol. 221, 2022, Art. no. 108330.

[15] E. Wang, H. Zhou, G. Wen, Z. Liu, and X. Chen, "Koopman-informed neural network for machinery's nonlinear dynamics learning and remaining useful life prediction," *IEEE Trans. Instrum. Meas.*, vol. 74, 2024, Art. no. 2502412.